# Organic & Biomolecular Chemistry



**REVIEW** 

View Article Online
View Journal | View Issue



**Cite this:** *Org. Biomol. Chem.*, 2020, **18**, 7238

# Synthesis strategies for non-symmetric, photochromic diarylethenes

Alvaro D. Sponza, Di Liu, Emily P. Chen, Allison Shaw, Lassana Diawara and Melanie Chiu 

\*\*Technology\*\* 
\*\*Technology\*\*

Diarylethenes (DAEs) represent an important class of photochromes with notable characteristics, like thermally irreversible photoisomerization and high fatigue resistance. Structural diversification of the DAE scaffold has enabled further refinement of photochromic properties and realization of new applications, ranging from advanced materials to tools for studying biological systems. In particular, methods for synthesizing non-symmetric DAE scaffolds, which are typically more challenging to synthesize than their symmetric counterparts, have grown over the past 20 years. These developments are surveyed in this review, with discussion of how access to these compounds has contributed to the improvement of photochromic properties and paved the way for exploring new applications of DAEs. First, non-symmetric DAE structures are classified and their uses and applications are overviewed. Subsequent sections discuss the main strategies that have been used to access non-symmetric DAEs with examples illustrating the impact of non-symmetric DAEs in the growing field of light-controlled molecular systems.

Received 29th July 2020, Accepted 8th September 2020 DOI: 10.1039/d0ob01556c rsc.li/obc

#### 1. Introduction

Diarylethenes (DAEs) were first highlighted in 1988 by Irie and co-workers as one of only a few classes of P-type photochromes, which are defined by thermally irreversible photo-

Department of Chemistry, Stony Brook University, Stony Brook, NY 11794, USA. E-mail: melanie.chiu@stonybrook.edu

isomerization. DAEs undergo a reversible, photochemical  $6\pi$ -electrocyclizaton between a ring-open and a ring-closed isomer (Scheme 1a). Generally, in the ring-open isomer, the aromatic rings are not electronically conjugated to one another because they are non-coplanar. Upon cyclization,  $\pi$ -conjugation extends across the bridge with concomitant dearomatization, resulting in substantial changes in molecular geometry and photophysical properties (Scheme 1a). In solu-



Alvaro D. Sponza

Alvaro D. Sponza received his Bachelor and Licentiate degrees from the Universidad Peruana Cayetano Heredia in 2013, under the mentorship of Profs. Norma Cuizano and Abel Navarro (CUNY Borough of Manhattan Community College), working on the evaluation of low-cost bioadsorbents for the removal of heavy metals pollutants from wastewater. He is currently a Ph.D. candidate in the research group of Prof. Melanie

Chiu at Stony Brook University, developing photoswitchable polymerization initiators.



Di Liu

Di Liu received his B.S. (2008) from Peking University and his M.S. (2010) from the University of Illinois, Chicago. He moved to the University of Texas, Austin to complete his Ph.D. (2016) under Profs. Christopher W. Bielawski and C. Grant Willson, where he developed post-polymerization modification of commodity plastics via direct C-H functionalization. After postdoctoral research in Prof. Willson's group developing and studying a new

aromatizing, self-immolative polyester, Di moved to Stony Brook University in 2017 to join Prof. Melanie Chiu's research group as a postdoctoral researcher exploring the use of remote stimuli to control polymer molecular weight distributions.

Scheme 1 (a) Reversible, photochemical  $6\pi$ -electrocyclization of a diarylethene. (b) Photoactive and photoinactive conformations of a ring-open diarylethene isomer.

tion, the ring-open isomer of a DAE can adopt two conformations: a photoactive one, in which the aryl groups are antiparallel to one another; and a photoinactive conformation, in which the aryl groups are parallel (Scheme 1b). The relative abundance of these two conformers dictates the quantum yield of the electrocyclization. The orientation of C1 and C1' in the antiparallel conformation (Scheme 1b) enables the electrocyclization and the conrotatory process results in the creation of two stereocenters, producing two ring-closed enantiomers (Scheme 1a).

Continued optimization of photochromic properties has expanded the usage of DAEs, with applications ranging from optoelectronic devices<sup>2,3</sup> to tools for super-resolution bioimaging.<sup>4</sup> Growing areas that feature DAEs include light-controlled homogeneous catalysis of small molecule reactions,<sup>5</sup> as well as supramolecular<sup>6–8</sup> and macromolecular systems.<sup>9–14</sup> Recent advances in DAE-containing supramolecular systems include catenanes and rotaxanes with photoswitchable components,<sup>6</sup> porphyrin complexes with photocontrolled release-and-report capabilities,<sup>7</sup> and a light-gated molecular motor.<sup>8</sup> Within the last decade, incorporating DAEs in polymers or

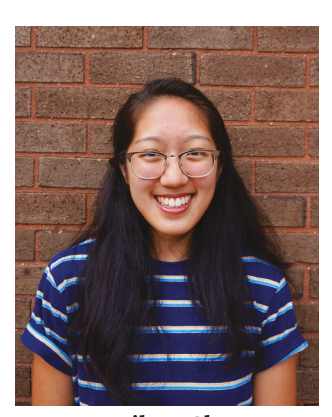
polymerization systems has enabled photocontrol of polymerization rate<sup>9,10</sup> or polymer dispersity,<sup>11</sup> optimization of optoelectronic properties in conjugated polymers,<sup>12</sup> and exploration of potential platforms for sensing mechanical stress in polymeric materials.<sup>13,14</sup>

Given the broad appeal of DAEs, a number of reviews have surveyed their applications<sup>15,16</sup> and structural diversity,<sup>17,18</sup> as well as their use in multi-responsive systems<sup>19</sup> and multi-photochromic systems.<sup>20,21</sup> However, focused review of synthetic strategies to access these scaffolds has been relatively rare.<sup>22</sup> Most surveys focus on symmetric DAEs; these are more commonly encountered due to their relative ease of access.<sup>15</sup> Yet, there are compelling motivations for synthesizing non-symmetric DAEs, such as access to bifunctional systems and fine control over the spatial orientation of constituent aryl groups to achieve desired photophysical properties (see section 2). This review focuses on synthetic strategies to access non-symmetric DAEs with a variety of aryl groups and cyclic bridges, and emphasizes developments since 2000 that have not previously been reviewed.

## 2. Uses of non-symmetric DAEs

The first non-symmetric DAE was reported by Irie and coworkers in 1995 as part of a systematic study of how photophysical properties of the closed isomers are affected by the position at which each thiophene ring is bound to the perfluorocyclopentene bridge (Scheme 2).<sup>23</sup> In these cases, substitution position affects the length of the conjugated systems in the closed isomers, and therefore, their absorption maxima.<sup>15</sup> Early efforts toward DAE-based, light-responsive materials also often required anchoring of non-symmetric, monofunctionalized DAEs to macromolecular substrates, such as polymers<sup>24,25</sup> and multilayer films.<sup>26</sup>

Access to non-symmetric DAEs facilitated fundamental studies on how the chemical reactivity of an appendant functional group is photochemically modulated due to changes in conjugation. The primary mode of control involves systems



Emily P. Chen

Emily P. Chen earned a B.E. in Chemical Engineering Stony Brook University (2020), where she undertook research in the groups of Profs. Nancy Goroff and Melanie Chiu, studying host-guest polymerization processes and optimizing controlled cationic polymerization reactions, respectively. She is currently a chemistry graduate student at theCalifornia Institute of Technology. Outside of the lab, Emily enjoys running, cooking, and baking.

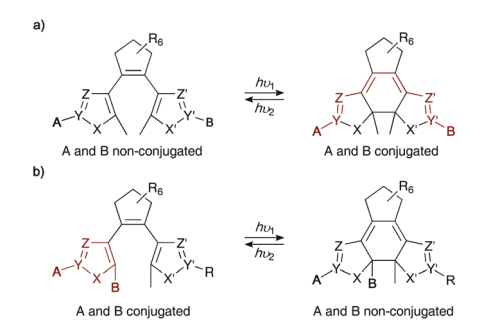


Allison Shaw

Allison Shaw is a junior in Chemical and Molecular Engineering at Stony Brook University, where she works as an undergraduate researcher in Prof. Melanie Chiu's group on studying the mechanisms of controlled cationic polymerization reactions. She is an avid traveler and community service volunteer.

$$\lambda_{\max} = 234 \text{ nm}$$
 $\lambda_{\max} = 312 \text{ nm}$ 
 $\lambda_{\max} = 336 \text{ nm}$ 

Scheme 2 Effect of the position at which thiophene rings are bound to the perfluorocyclopentene bridge on  $\lambda_{\text{max}}$  of DAE closed isomers.



**Scheme 3** Changes in electronic communication between substituents A and B upon photoelectrocyclization when: a) substitutents are appended to different aryl groups; and b) when substitutents are appended to the same aryl group.

where two functionalities are attached to different aryl groups, and ring-closing results in enhanced electronic communication between them (Scheme 3a). In another scenario, two functionalities are located on the same aryl group, and ringclosing results in decreased electronic communication between them (Scheme 3b). These systems have enabled photocontrol over chemical reactivity, including Brønsted

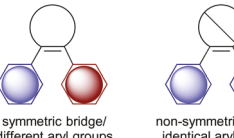


Fig. 1 Classification of non-symmetric DAEs.





symmetric bridge/ different aryl groups non-symmetric bridge/ identical aryl groups

acidity (section 5.1), 11,27,28 Lewis basicity (section 5.1), 29,30 and electrophilicity (section 3.1), 31,32 as well as the rate of release of small molecules (section 5.3).33

Non-symmetric DAEs have also been used to tune the torsional angle between the aryl groups. This control over the relative spatial arrangement of DAE substituents has been exploited to optimize cyclization quantum yields  $(\phi_{o-c})$  by stabilizing the photoreactive, antiparallel conformation via intramolecular, non-covalent interactions (section 3.2).34-36 Such DAEs often exhibit other desirable photochromic properties, such as high fatigue resistance and thermal stability. 15 Finally, the spatial control afforded by non-symmetric DAEs has also been used to induce stereoselective electrocyclizations (section 3.1).37-40

In the following sections, we discuss the main synthetic strategies that have been used for the synthesis of non-symmetric DAEs. We classify non-symmetric DAEs into three structural types as illustrated in Fig. 1: (a) two different aryl groups attached to a symmetric bridge (left); (b) two identical aryl groups attached to a non-symmetric bridge (middle); and (c) two different aryl groups attached to a non-symmetric bridge (right). These three types of non-symmetric DAEs have been accessed using three main synthetic strategies: (a) consecutively coupling aryl groups to a symmetric or non-symmetric bridge precursor (Scheme 4a); (b) ring-closing a diaryl intermediate in an intra- or intermolecular fashion (Scheme 4b); and (c) desymmetrizing a symmetric DAE or DAE precursor (Scheme 4c). Each of these strategies are discussed below, with examples of their recent applications in achieving notable photochromic properties or chemical reactivity.



Lassana Diawara

Lassana Diawara earned his B.S. in Chemistry from St John's University (2019) where he worked in the laboratory of Prof. Robin Hyslop on the synthesis and characterization of porphyrin complexes. He is a graduate student with Prof. Melanie Chiu working on developing efficient methods for the synthesis of block copolymers with varying block dispersities. Aside from chemistry, Lassana enjoys basketball and listening to music.



Melanie Chiu

Melanie Chiu earned her A.B. (2004) from Dartmouth College and her Ph.D. (2009) from the University of California, Berkeley with Profs. Robert G. Bergman and F. Dean Toste. After postdoctoral research with Prof. Dr François Diederich at ETH Zürich and Prof. Zhenan Bao at Stanford University, she began her independent career at Stony Brook University in 2014. Her research group develops methods that utilize external stimuli to

exert precise control over polymer molecular weight distributions and copolymer microstructures.

Scheme 4 Synthesis strategies for non-symmetric DAEs: (a) coupling of arvl groups to bridge precursors: (b) intramolecular (left) or intermolecular cyclization (right) of diaryl intermediates; and (c) modification of a symmetric intermediate by functionalizing one aryl group (left) or the bridge (right).

### Coupling aryl groups to a bridge precursor

#### 3.1. Substitution of octafluorocyclopentene using aryllithiums

The hexafluorocyclopentene bridge is incorporated into DAEs because the resulting compounds often exhibit high fatigue resistance and thermal stability. 16,41 Non-symmetric DAEs incorporating the hexafluorocyclopentene bridge are usually prepared by sequentially attaching two distinct aryl groups to commercially available octafluorocyclopentene via nucleophilic substitution (Scheme 5).

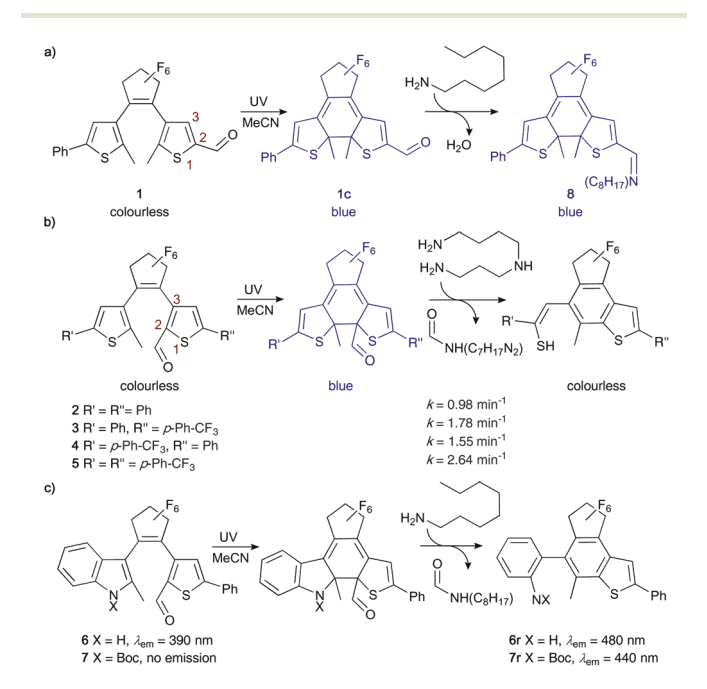
The first substitution usually results in a mixture of monoand disubstituted products, and to maximize the yield of the desired monosubstituted product, an excess of octafluorocyclopentene is often used. This can be disadvantageous, given the high cost and volatility of octafluorocyclopentene (bp = 27 °C). Additionally, electrophilic or acidic functional groups on the aromatic rings, such as carbonyl32 and hydroxyl groups,42 must be protected prior to lithiation. Despite these drawbacks, this method has been a workhorse for accessing DAEs the hexafluorocyclopentene bridge variety of aryl groups attached. Furthermore, this method is amenable to implementation in a flow microreactor system.<sup>43</sup> Representative examples of arenes that incorporated into DAEs using the sequential substitution method include pyrrole, 44 thiazole, 44-46 benzosilole,47 pyridine,44,48 indazole,49 pyrimidine,50 benzopyrrole,<sup>32</sup>

$$\underbrace{ \begin{matrix} \begin{matrix} F_6 \\ F \end{matrix} }_F + Ar^1-Li & \longrightarrow \underbrace{ \begin{matrix} \begin{matrix} F_6 \\ Ar^1 \end{matrix} }_F + Ar^2-Li & \longrightarrow \underbrace{ \begin{matrix} \begin{matrix} F_6 \\ Ar^2 \end{matrix} }_A + Ar^2-Li \\ Ar^2-Li \end{matrix} }_Ar^2$$

Scheme 5 Sequential nucleophilic substitutions of octafluorocyclopentene with aryllithiums.

benzofuran, 32,47 benzothiophene, 32,47,51 benzene, 32,44 and isoxazole. 42,52 In general, the two arvl groups can be appended to the bridge in either order, but the second substitution reaction typically proceeds in lower yields (<50%). Aryl groups bearing functional groups that are tolerated, such as ferrocene,<sup>53</sup> alkyne,<sup>53</sup> nitrile,<sup>44</sup> tertiary amines,<sup>32</sup> and ethers,<sup>37,38,40</sup> can be directly coupled with the bridge.

The versatility of this synthetic tactic has enabled systematic studies on how reactivity of a given functional group changes upon photoelectrocyclization. For example, in the development of photoswitchable sensors, Hecht and coworkers prepared a series of aldehyde-substituted DAEs and evaluated the effect of photoisomerization on their reactivity with amines.32 Some of the non-symmetric DAEs used in this study (1-7, Scheme 6) were prepared by coupling protected arylaldehydes to monoarylated heptafluorocyclopentene intermediates. The closed DAE isomers reacted differently depending on the position of the aldehyde group. When the aldehyde functionality was located at the outer 2-position (1, Scheme 6a), reaction with octylamine resulted in the formation of imine 8. In contrast, when the aldehyde was located at the inner 2-position (2-5, Scheme 6b) and treated with spermidine, the proposed hemiaminal intermediate underwent fragmentation to yield colourless products. The rate of amineinduced reaction could be accelerated by placing an EWG close to the aldehyde functionality (3), at the other aryl group (4), or a combination of both (5). Finally, DAEs 6 and 7 demon-



Scheme 6 Variations in reactivity according to the substitution position. Photoelectrocyclization followed by: (a) imine formation after reacting aldehyde located at the outside 2-position with octylamine; or (b) amine-induced fragmentation after reacting aldehyde located at the inside 2-position with spermidine. (c) Changes in fluorescence properties upon light-induced fragmentation of closed aldehyde-DAEs in the presence of amines.

strated potential as a platform for fluorescence-based sensors, as their fragmentation products, **6r** and **7r**, exhibited changes in their fluorescence spectra (Scheme 6c).

The aromaticity of the aryl groups has important effects on the thermal stability of closed DAE isomers. The thermal stability of the closed isomer of a symmetric DAE decreases when the aromatic stabilization energies (ASEs) of its constituent aryl groups increase. This correlation also holds in non-symmetric DAEs, as demonstrated in the series of pyrrole-containing DAEs (9–13, Scheme 7). The closed isomer of symmetric DAE 9 exhibited poor thermal stability (50% thermal electrocyclic ring-opening after 37 s at rt) relative to non-symmetric scaffolds, each incorporating one aryl group with lower ASE (10 and 11, no thermal electrocyclic ring-opening observed after 400 s at 20 °C). On the other hand, non-symmetric DAEs incorporating one aryl group of higher ASE (12 and 13) showed ~30% and >99% thermal electrocyclic ring-opening after 400 s and 150 s, respectively, under the same conditions.

Symmetric DAEs incorporating aryl groups with low ASEs typically exhibit modest photochromic properties, but replacement of one arvl group with a group of higher ASE to form a non-symmetric DAE can sometimes result in enhanced photochromic properties, such as increased cyclization quantum yield, ring-opening quantum yield, or fatigue resistance (Fig. 2).55 For example, while symmetric dithiazole 14 exhibited a  $\phi_{\rm o-c}$  value of 0.16,<sup>56</sup> a much higher value,  $\phi_{\rm o-c}$  = 0.42, was measured for non-symmetric DAE 15 containing a phenyl group.<sup>57</sup> Similarly, while symmetric DAE **16** exhibited a  $\phi_{c-0}$ value of 0.013, non-symmetric DAE 17, containing a pyrimidine group (high ASE), exhibited a  $\phi_{c-0}$  value of 0.26.<sup>50</sup> Improvement in fatigue resistance by tuning aryl group ASEs is exemplified by comparing symmetric DAE 18 vs. non-symmetric DAE 19. While DAE 18 underwent ~50% decomposition after 10 UV/Vis irradiation cycles DAE 19, which incorporates a high ASE pyridine group, underwent 12 irradiation cycles with less than 1% decomposition.48

Non-symmetric DAEs also present an opportunity to study stereoselectivity in DAE photoelectrocyclization. Yokoyama and co-workers prepared a variety of non-symmetric, enantio-enriched DAEs in which the constituent thiophenes were functionalized with point (20),<sup>38</sup> axial (21)<sup>37</sup> and planar (22)<sup>40</sup> chiral substituents (Fig. 3). These chiral substituents were

**Scheme 7** Effect of aromatic stabilization energies of the aryl groups on the thermal stability of closed DAEs isomers.

Fig. 2 Effect of combining aryl groups with different aromatic stabilization energies on the photoelectrocyclization quantum yield and fatigue resistance of DAE closed isomers. Quantum yield measurements were performed in n-hexane.

Fig. 3 Chiral DAEs that undergo diasteresoselective photoelectrocyclization. de $_{\rm o-c}$  = diastereomeric excess of photoelectrocyclization product.

installed on the thiophenes prior to attachment to the octafluorocyclopentene bridge and were unaffected by the nucleophilic substitution. Typically, the cyclization of DAEs produces a mixture of two enantiomers in a ratio that reflects the population distribution of the two antiparallel, helical conformers. The presence of a chiral group on the DAE scaffold introduces a bias in the ratio of the two conformers, resulting in a diastereoenriched closed isomer upon cyclization. Steric bias can be introduced by 1,3-allylic strain, as in DAEs 20 and 21, resulting in diastereomeric excesses (des) of 88% and 90%, respectively. In planar chiral DAE 22, the bulky triethyleneglycol (Teg) bridge attached to one of the thiophene rings prevents approach of the other thiophene from the bridge face. Therefore, only one antiparallel conformer was able to undergo cyclization with 100% de and 88% conversion.

#### 3.2. Palladium cross-coupling of bridge precursors

Despite the variety of aryl groups that can be incorporated in non-symmetric DAEs using the nucleophilic substitution method described previously, the bridge precursor is limited to octafluorocyclopentene, which is electron-deficient enough to undergo substitution reactions. In contrast, palladium-catalyzed cross-coupling methods expand the types of bridges that can be incorporated (Scheme 8). We can classify the products obtained using this method into three types based on their bridge architectures: (a) symmetric (Scheme 8a); (b) non-symmetric (Scheme 8b); and (c) functionalizible bridges (Scheme 8c). Suzuki cross-coupling is the most commonly

**Scheme 8** Synthetic approaches to access DAEs with (a) symmetric; (b) non-symmetric; and (c) functionalizible bridges.

used transformation, where vinyl or aryl dibromides are typical bridge precursors. However, cycloketones can also serve as bridge precursors when used in combination with other coupling strategies. Bridge units incorporated using cross-coupling reactions include thiazole, benzothiophene, benzothiophene, azaindole, thiophene, furan, benzindenone, benzindenone, cyclopentene, and cyclohexene.

DAEs with symmetric bridges (Scheme 8a) accessed by Suzuki cross-coupling are exemplified by nucleoside-functionalized DAE 23 <sup>64</sup> and oligonucleotide-functionalized DAE 24 (Scheme 9). <sup>65</sup> As shown in Scheme 9a, the preparation of these compounds commences with the coupling of arylboronic ester 25 with 1,2-dibromocyclopentene, followed by borylation of the resultant monoarylated bromocyclopentene 26. The resulting boronic ester 27 is coupled with aryl iodide 28 or 29 to yield the final products. Use of this strategy is necessary due to the incompatibility of intermediate 28 with organolithiums used in the nucleophilic substitution strategy. Preliminary evi-

dence suggests that nucleoside-functionalized DAE 30, derived from DAE 23, forms a hydrogen-bonded complex with thymidine (Scheme 9b). Gel electrophoresis experiments qualitatively imply that double-stranded DNA incorporating the closed isomer derived from oligonucleotide-functionalized DAE 24 undergoes transcription at a slower rate than the counterpart incorporating the corresponding open isomer (Scheme 9c).

Suzuki cross-coupling has also permitted the incorporation of non-symmetric bridges (Scheme 8b), which have led to remarkably high cyclization quantum yields. This outcome is due to the fact that a given DAE exists in solution as an equilibrium mixture of conformational isomers: an antiparallel conformer that is photoactive, and a parallel conformer that is photoinactive (Scheme 1b). For symmetric DAEs, the relative abundance of these isomers is typically 1:1, from which a maximum  $\phi_{o-c}$  of 0.5 is expected. However, non-symmetric DAEs introduce a bias in the relative abundance of conformational isomers by stabilizing the photoreactive, antiparallel via intramolecular, non-covalent interactions,  $^{34-36,58-60}$  leading to  $\phi_{\mathrm{o-c}}$  values above 0.5. Kawai and co-workers illustrated this concept using a series of DAEs, 31-34, in which non-symmetric bridges are thought to participate in non-covalent, intramolecular interactions to stabilize the antiparallel conformer and increase its population in solution (Fig. 4). The higher cyclization quantum yield of DAE 32 compared to DAE 31 ( $\phi_{\text{o-c}}$  = 0.6 and 0.4, respectively) was attributed to the presence of a CH2-H···N-H stabilizing interaction.<sup>58</sup> Using a benzothiophene bridge, as in DAE 33, was postulated to enable a stronger putative S...N heteroatomcontact interaction<sup>68</sup> and N···H hydrogen bonding, which resulted in an extraordinarily high cyclization quantum yield  $(\phi_{\text{o-c}} = 0.98 \text{ in } n\text{-hexane}).^{35} \text{ A high cyclization quantum yield}$  $(\phi_{\text{o-c}} = 0.90)$  in a polar solvent (methanol) was reported for the first time by using non-symmetric DAE 34,60 featuring N···H and CH2-H...N intramolecular hydrogen bonding between the bridge and aryl groups. Similar stabilization effects were

Scheme 9 (a) Nucleoside (23) and oligonucleotide (24)-functionalized DAEs synthesized by sequential coupling of aryl groups to 1,2-dibromocyclopentene. (b) Base-pair formation of DAE 23 with thymidine. (c) Light-induced change in the transcription rate of dsDNA incorporating DAE 24.

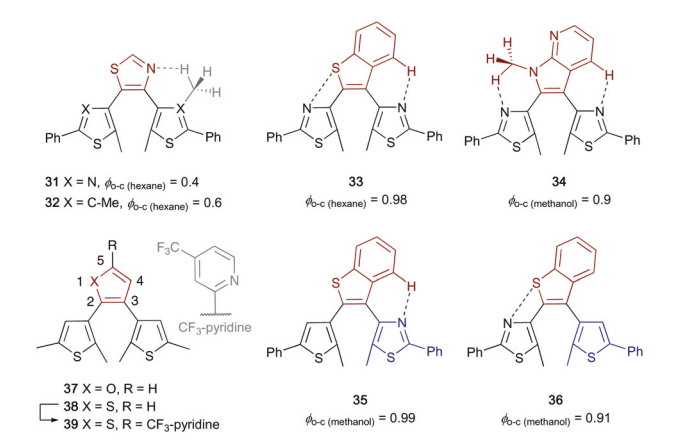


**Fig. 4** DAEs prepared by coupling aryl groups to a non-symmetric bridge.

observed in the regioisomeric pair, 35 and 36, with  $\phi_{o-c}$  = 0.99 and 0.91 in methanol, respectively (Fig. 4).<sup>59</sup>

Non-symmetric DAEs 37 and 38 (Fig. 4) are examples of functionalizible DAE bridges (Scheme 8c), as reported by Yam and co-workers. These compounds possess a 2,3-substituted furan<sup>62</sup> or thiophene bridge<sup>61</sup> (Fig. 4), which could be further derivatized at the reactive 5-position to achieve extension of  $\pi$ -conjugation or attachment of chelating agents.<sup>61,69,70</sup> For example, *p*-trifluoromethylpyridine-substituted DAE 39 was

used for the formation of a platinum(II) complex where the ring-closed isomer exhibited near-infrared absorption. <sup>61</sup>

Cycloketones can be incorporated as bridges using the approaches depicted in Schemes 10a and b. For example, palladium-catalyzed α-arylation of cyclopentanone with aryl bromide 40 produced monocoupled intermediate 41, which was subsequently transformed into triflate 42 (Scheme 10a).9 Pinacol ester 43 underwent cross-coupling with triflate 42 in the final step, producing DAE 44. Methoxy-substituted DAE 44 was converted to the photoswitchable hydroxy-substituted DAE 45, whose ring-closed isomer, 45c, rapidly tautomerizes into the more stable ketone, 45k (Scheme 10c). This light-induced keto-enol tautomerization was exploited to control the rate of ring-opening polymerization of L-lactide using light. When DAE 45 was used as a catalyst, monomer activation was possible via hydrogen bonding, but the absence of a hydrogenbond donor in DAE 45k made it an inactive catalyst. Using these catalysts in the copolymerization of  $\delta$ -valerolactone (VL) and trimethylcarbonate (TMC) enabled photocontrol of monomer reactivity ratios. While use of DAE 45 yielded a random copolymer with greater VL incorporation, use of DAE 45k favored TMC incorporation.

 $\alpha$ -Arylation was also used to access chiral DAE 46 (Scheme 10b), in which the resulting diastereomeric outcome upon photoelectrocyclization could be manipulated by taking advantage of the differences in absorption profile and acid stability between the closed diastereomers 46a and 46b

Scheme 10 Sequential addition of aryl groups to (a) cyclopentanone and (b) L-menthone. (c) Photocontrol of the rate of polymerization in the ring-opening polymerization of L-lactide, and monomer incorporation in the random copolymerization of  $\delta$ -valerolactone and trimethylcarbonate. (d) Switchable photoelectrocyclization diastereoselectivity. dr = diastereomeric ratio.

Scheme 11 Synthesis of DAEs via intramolecular McMurry reaction of a non-symmetric diketone intermediate. Diketone intermediates obtained either by (a) sequential Friedel–Crafts reactions or (b) nucleophilic substitution followed by oxidation.

(Scheme 10d).<sup>67</sup> DAE **46** was prepared by α-arylation of L-menthone with bromide **47**, followed by nucleophilic addition of ketone **48** with lithiated derivative of bromide **47**. Chlorination of the resulting alcohol, **49**, and subsequent elimination generated the bridge double bond. Upon UV irradiation, DAE **46** formed diastereomer **46b** with a diastereomeric ratio (dr) of 85:15. In contrast, UV irradiation of **46**, either under acidic conditions or with simultaneous red light irradiation, produced diastereomer **46a** with diastereomeric ratios of 99:1 and 74:26, respectively. In these latter scenarios, the inversion in diastereoselectivity is due to the fact that TFA and red light preferentially open diastereomer **46b** over **46a**, leading to an accumulation of **46a** over time. This system is a rare example of light-driven chiral resolution.

# 4. DAE bridge formation *via* ring-closing reaction

In the strategies discussed previously, non-symmetric DAEs are prepared by attaching aryl groups to a cyclic bridge precursor. Another strategy involves the transformation of a diaryl precursor to form the bridge in a convergent fashion. Notably, compounds with unusual bridges have been obtained using this strategy. Below, we present the two main examples of this ringforming strategy: the intramolecular cyclization of diaryldiketones (sections 4.1 and 4.2) and the intermolecular cyclization of diarylacetylenes (section 4.3).

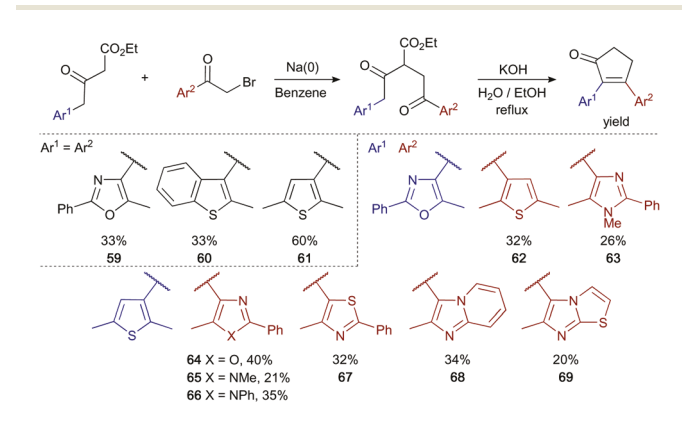
#### 4.1. Intramolecular McMurry reaction of diaryldiketones

Intramolecular McMurry coupling of 1,5-diaryl-1,5-diketones is an established strategy to access symmetric DAEs.<sup>71</sup> This strategy was used to access non-symmetric DAEs **50** and **51** from diaryldiketone intermediates **52** and **53**, respectively (Scheme 11a).<sup>72</sup> These key intermediates were prepared using two consecutive Friedel–Crafts reactions between glutaric anhydride and the corresponding arenes. DAE **51** was the first example of a cyclopentene-bridged DAE that exhibited single crystal photochromism. Access to the diarylketone intermediate is not limited to Friedel–Crafts disconnections. An alterna-

tive synthesis of the diaryldiketone intermediate is exemplified in the synthesis of DAE 54 (Scheme 11b).<sup>73</sup> Reaction of thienyl lithium 56 with hemiacetal 55 was followed by treatment with PPh<sub>3</sub>=CH<sub>2</sub> and oxidation of the corresponding diol, 57 to form diaryldiketone 58. These compounds represent the first uses of the intramolecular McMurry reaction to access nonsymmetric DAEs.

#### 4.2. Aldol condensation

DAEs with bridges that are either five- or six-membered rings can be accessed using intramolecular aldol condensation. The key diketone intermediates are prepared from: (a)  $\beta$ -ketoesters and bromomethyl aryl ketones for accessing cyclopentenone-bridged DAEs **59–69** (Scheme 12);<sup>74–76</sup> and (b)  $\beta$ -ketoesters and  $\alpha,\beta$ -unsaturated ketones for accessing cyclohexenone-bridged DAEs **70–75** (Scheme 13).<sup>77</sup> The  $\beta$ -ketoester and bromomethyl aryl ketone precursors for these reactions are easily prepared from commercially available, inexpensive aryl methyl ketones. The aryl groups that have been incorporated using this method include thiophene, <sup>74,75,77</sup> benzothiophene, <sup>74</sup> thiazole, <sup>76</sup> oxazole, <sup>75,77</sup> imidazole, <sup>77</sup> imidazo[1,2- $\alpha$ ]pyridine, <sup>76</sup> and imidazo[2,1- $\alpha$ ]thiazole. <sup>76</sup> The presence of the carbonyl group on the bridge enables further functionalization. <sup>74,75</sup> In



Scheme 12 Synthesis of cyclopentenone-bridged DAEs by reaction of bromomethyl aryl ketones and  $\beta$ -ketoesters and subsequent aldol condensation.

Scheme 13 Synthesis of cyclohexenone-bridged DAEs by reaction of  $\alpha,\beta$ -unsaturated ketones and  $\beta$ -ketoesters and subsequent aldol condensation.

Scheme 14 Reduction of cycloketone-bridged DAEs.

addition, reduction with triethylsilane under acidic conditions yielded cycloalkene-bridged DAEs (Scheme 14),76 expanding the scope of cycloalkene-bridged DAEs that can be accessed compared to those that can be obtained via intramolecular McMurry reaction.

#### 4.3. Coupling of diarylacetylenes

Transition-metal catalyzed/mediated intermolecular cyclization of diarylacetylenes is an attractive method to access non-symmetric DAEs because the precursors can be conveniently prepared by Sonogashira reaction. This method has mainly been used to prepare structures where identical aryl groups are appended to a non-symmetric bridge. DAEs with silole,78 phosphole, 79-82 indenone 83 and metallacycle 84 bridges have been accessed using this approach.

In an early example, non-symmetric DAEs 76 and 77 featuring an indenone bridge were obtained via palladium-catalyzed coupling of diarylacetylenes 78 and 79, respectively, with arylboronic acid 80 (Scheme 15a).83 Surprisingly, DAE 77 exhibited a low  $\phi_{o-c}$  value of 0.1, despite the proposed presence of a C-H...N stabilizing interaction. Modification of the carbonyl group yielded spiro-DAEs 81 and 82, for which higher  $\phi_{o-c}$ values have been measured (0.8 and 0.98, respectively), relative to the non-spiro precursor, 77 (Scheme 15b).85 These effects have been attributed to two factors: (a) introduction of a second stabilizing C-H···N intramolecular interaction for DAE 81; and (b) steric hindrance between the substituent on the bridge and one of the thiazole groups for DAE 82, which was proposed to stabilize the antiparallel conformation. Similar effects have been observed in other DAEs with bulky bridge substituents.86

The first example of a DAE incorporating a silole bridge, DAE, 83 was reported by Yam and coworkers. This compound

Scheme 15 (a) Synthesis of an indenone-bridged DAE. (b) Derivatization of DAE 76 into spiro-functionalized DAEs with higher photoelectrocyclization quantum yields

Scheme 16 Synthesis of a benzosilole-bridged DAE by coupling a diarylacetylene with a silylaryl bromide.

was prepared by coupling dithienylacetylene 84 with silane 85 (Scheme 16)<sup>78</sup> via an unusual Si-C activation pathway.<sup>87</sup> The  $\phi_{\text{o-c}}$  value measured for DAE 83 was 0.48, which approaches the theoretical maximum for a DAE lacking stabilizing intramolecular interactions; the corresponding photoelectrocyclic ring-opening quantum yield ( $\phi_{c-o} = 0.42$ ) is high compared to those typically measured in DAEs (<0.10). Notably, DAEs that exhibit  $\phi_{\text{o-c}}$  and  $\phi_{\text{c-o}}$  values that are both similar and high are very uncommon. This parity is important in certain photochromic applications, such as memory devices.

The incorporation of phosphine oxide units in DAE bridges has been achieved by dehydrogenative annulation of phenyl hydrophosphine oxides with diarylacetylenes (Scheme 17a), resulting in DAEs 86-95. 79-82 An attractive property of DAEs with a phosphole oxide bridge is their visible light photochromism. Conventionally, visible light photochromism is achieved by extending the  $\pi$  system at the DAE aryl groups, but this results in reduction of both  $\phi_{\rm o-c}$  and  $\phi_{\rm c-o}$  values (<0.01). In contrast, DAEs 89-94 possess extended  $\pi$ -conjugation at the phosphole bridge, and these underwent cyclization upon

Scheme 17 (a) Synthesis of phosphole-bridged DAEs by coupling diarylacetylenes with phosphine oxides. (b) Thionation of DAE 95 into DAE 96 with higher  $\phi_{\rm o-c}$  and  ${\rm de_{o-c}}$  values.  ${\rm de_{o-c}}$  = diastereomeric excess of photoelectrocyclization product.

irradiation at ca. 407 nm (violet), with relatively high  $\phi_{\rm o-c}$  values (0.23 to 0.87). Additionally, high  $\phi_{\rm c-o}$  values were measured for some of these compounds (0.084 to 0.44). Furthermore, phosphole oxide bridged DAE 95 could be converted to phosphole sulfide 96 (Scheme 17b), which resulted in an increased cyclization quantum yield ( $\phi_{\rm o-c}=0.47$  for 95 and  $\phi_{\rm o-c}=0.98$  for 96), <sup>82</sup> as well as an increased cyclization diastereoselectivity ( ${\rm de_{o-c}=50\%}$  for 95 and  ${\rm de_{o-c}=67\%}$  for 96). Exploring the regioselectivity of this transformation and its impact on photochromic properties could provide further design insights for DAEs with heteroatom-containing bridges. <sup>88</sup>

Finally, Wolf and co-workers prepared the first DAE with a metallacyclobutene bridge<sup>84</sup> *via* zirconaphosphination of diarylacetylene **97** (Scheme 18a). Zirconacycle **98** served as an intermediate for the preparation of a series of copper(i) complexes containing diarylethene-based bidentate phosphine ligands. These are the first examples of a transition metal incorporated into the bridge of a photoactive DAE. Dinuclear copper(i) complex **99** (Scheme 18b) served as a pre-catalyst in the copper(i)-catalyzed hydroboration of alkenes (Scheme 18c). Preliminary observations indicated that the ring-open isomer of DAE copper complex **100** is a more active catalyst than the ring-closed isomer, **100c**.

# 5. Modification of a symmetric intermediate

Complementary to direct formation of non-symmetric DAE scaffolds, symmetric DAE intermediates can be modified to

Scheme 18 (a) Synthesis of a metallacycle-bridged DAE by metallophosphination of a diarylacetylene. (b) Synthesis of a dinuclear copper pre-catalyst and (c) its use in the photocontrolled copper-catalyzed hydroboration of styrenes.

access non-symmetric products. This desymmetrization strategy takes advantage of many existing methods to synthesize symmetric DAEs, and can be used to access DAEs that feature either modified bridges or aryl groups that incorporate different substituents. Here, we present three commonly used approaches for the desymmetrization of symmetric intermediates. The first two approaches involve derivatization of the aryl groups, and the last approach features modification of the bridge.

#### 5.1. Selective functionalization of one DAE aryl group

Selective functionalization of one of the DAE aryl groups is one of the most widely used approaches for DAE desymmetrization.<sup>22</sup> For instance, a monolithiated intermediate generated by lithium-halogen exchange is trapped by an electrophile, such as B(OR)3,89 DMF,22,31 or PPh2Cl.30 This method has been commonly used for derivatizing cyclopentene-bridged DAEs with thiophene rings. The yields of products derived from monolithiated intermediates for DAEs with fluorinated bridges typically range from 50 to 60%. Corresponding yields for DAEs with non-fluorinated bridges tend to be higher (70-80%). Depending on the nature of the trapping electrophile, the final monofunctionalized product may be difficult to separate from the symmetric, bifunctionalized byproduct and the unreacted starting material. Nevertheless, a large number of non-symmetric, bifunctional DAEs have been obtained using this method and are employed in numerous applications, such as photomodulation of Lewis basicity, 30 Brønsted acidity<sup>11</sup> and supramolecular assembly.<sup>90</sup>

Desymmetrization of DAE **101** *via* lihiation–phosphination, or lithiation–boronation and subsequent functionalization,

a)

R' = Cl

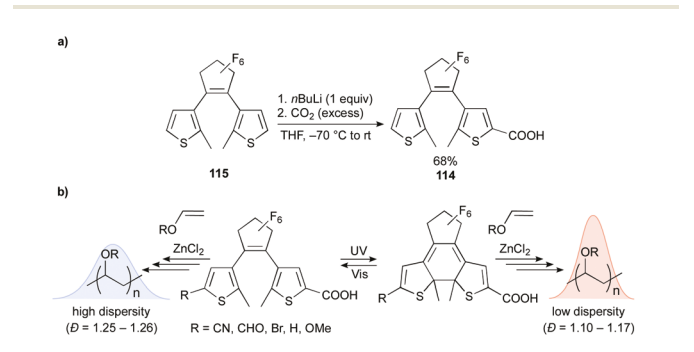
1. 
$$/BuLi$$
2.  $B(OBU)_3$ 
3.  $Pd(PPh_3)_4$ 
6.  $K_2CO_3$ 
4.  $K_3CO_3$ 
4

Scheme 19 (a) Synthesis of phosphine-substituted DAEs and (b) their photocontrolled Lewis basicity.

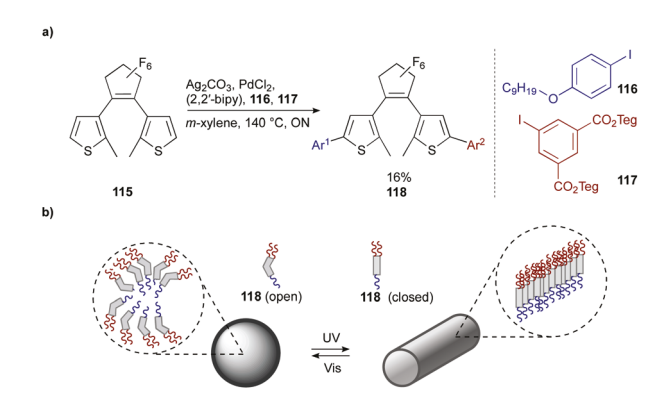
113  $\Delta^{1}J_{P-Se} = 5 \text{ Hz}$ 

yielded DAEs 102-103, and 104-107, respectively, which bear a diphenylphosphino group (Scheme 19a).30 The effect of the photoelectrocyclization of DAEs 102-107 on the σ-donating ability of the phosphine was studied by preparing the corresponding phosphine selenides, 108-113, and analyzing the change of the P-Se coupling constant upon ring-closure (Scheme 19b,  $\Delta^1 J_{P-Se}$ ). All selenides exhibited a positive  $\Delta^{1}J_{P-Se}$ , indicating reduced  $\sigma$ -donating ability of the corresponding phosphines upon ring-closure. Moreover,  $\Delta^1 J_{P-Se}$ increased with the electron-withdrawing ability of the peripheral substituents of the DAE scaffold.

Similarly, our group recently reported a series of substituted DAE carboxylic acids derived from parent monocarboxylated DAE 114, accessed via lithiation of symmetric DAE 115 and trapping with CO<sub>2</sub> (Scheme 20a). 11 DAE 114 and its derivatives were studied as initiators for the cationic polymerization of vinyl ethers (Scheme 20b). It was found that polymers obtained using the ring-open isomers as initiators exhibited higher dis-



Scheme 20 (a) Synthesis of DAE carboxylic acid precursor. (b) Use of DAE carboxylic acids as initiators for the cationic polymerization of vinyl ethers to achieve photomodulation of polymer dispersity.



Scheme 21 (a) One-pot synthesis of amphiphilic DAE via direct C-H activation of a symmetric DAE precursor. (b) Photoswitchable microphase behaviour. Teg = triethyleneglycol.

persities than those obtained with ring-closed isomers. This change was attributed to the formation of a less nucleophilic carboxylate upon ring-closure, which was exploited to achieve photocontrol of the polymer dispersity for the first time.

The introduction of new functionalities on a DAE scaffold via direct C-H arylation is an attractive strategy that has seldom been reported. 90,91 One example is the functionalization of DAE 115 with aryl halides 116 and 117, used to prepare amphiphilic, non-symmetric DAE 118 in a one-pot reaction (Scheme 21a).90 When dispersed in water, DAE 118 self-assembled into microspheres that underwent a reversible phase transition to form fibers upon irradiation with UV light (Scheme 21b). The morphological change was attributed to the loss of flexibility in DAE 118 upon photoisomerization to a more rigid and planar, ring-closed isomer, which exhibited stronger  $\pi$ - $\pi$  stacking.

#### 5.2. Oxidation of a heteroaryl group

For DAEs containing heteroaryl rings, desymmetrization can be accomplished by heteroatom oxidation. One example of this strategy is the oxidation of symmetric DAEs 119 and 120 using mCPBA to afford monofunctionalized S,S-dioxide DAEs 121 and 122, respectively (Scheme 22a). 92 DAEs 121 and 122 exhibited higher fatigue resistance (~7 times) compared to symmetric DAE precursors 119 and 120, as well as their bis-oxidized analogues. The higher stability of 122 over 121 (~10 times) can be attributed to the instability of monofunctionalized S,S-dioxide DAEs bearing thiophene groups, which can release SO<sub>2</sub> upon UV irradiation. 93,94 Using a similar approach, oxidation of symmetric DAE 123 with diacetoxyiodobenzene in the presence of ammonium carbonate produced DAE 124 bearing a sulfoximidoyl group (Scheme 22b).95 This latter transformation produced no detectable quantities of the bisoxidized product, even when excess oxidant was added. In contrast to a sulfonyl group, the sulfoximidoyl group can be further functionalized. Acetylation of DAE 124 proceeded in 98% yield and the resulting DAE, 125, exhibited improved

Scheme 22 (a) Synthesis of S,S-dioxide DAEs by oxidation with mCPBA. (b) Synthesis of sulfoximine DAEs by oxidation with diacetoxy-iodobenzene in the presence of ammonium carbonate.

cyclization quantum yield ( $\phi_{\rm o-c}$  = 0.0063 for DAE 124,  $\phi_{\rm o-c}$  = 0.36 for DAE 125).

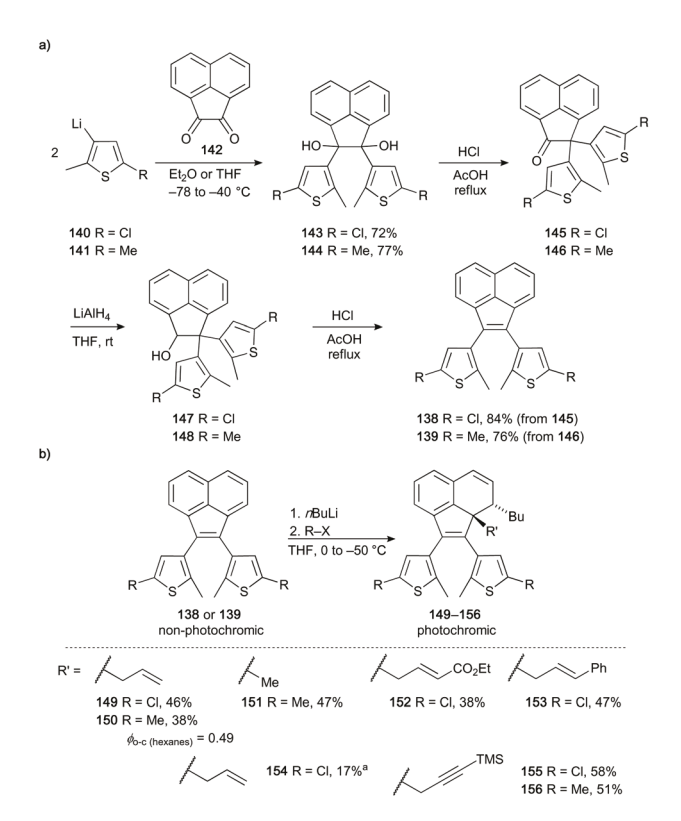
#### 5.3. Bridge desymmetrization

Apart from the derivatization of the aryl groups, desymmetrization of DAEs can be achieved by modifying the bridge unit. Here, we present three bridges and the corresponding transformations that can be used to desymmetrize them: N-substitution of imidazoles, addition to acenaphthylenes, and [4+2] cycloaddition of dienes.

N-Alkylation and transition-metal catalyzed N-arylation have been used to functionalize imidazole-bridged DAEs, which are functionally symmetric because they exist as mixtures of degenerate tautomers. The general strategy for preparing these symmetric precursors is exemplified in the synthesis of DAE 126 (Scheme 23a). Diketone 127, obtained via Friedel-Crafts acylation of 2,5-dimethylthiophene with oxalyl chloride, was reacted with formaldehyde and ammonium acetate in one-pot to form DAE 126. Desymmetrization is possible by selectively functionalizing one of the nitrogen atoms. For example, Yam and co-workers prepared N-alkylated DAEs 128 and 129 from DAE 126 and alkyl halides 130 and 131, respectively (Scheme 23b). 96,97 The same group also reported a series of N-arylated, imidazole-bridged DAEs, 132-137, which were prepared by copper(1)-catalyzed cross-coupling of DAE 126 with electron-deficient aryl halides (Scheme 23c). These non-symmetric imidazole-bridged DAEs were used for the formation of photochromic, N-heterocyclic carbene-ruthenium(II) complexes.

Guanti and co-workers reported the desymmetrization of an acenaphthylene-bridged DAE (Scheme 24). The synthesis of symmetric, non-photochromic acenaphthylene-bridged DAEs 138 and 139 commenced with the nucleophilic addition of lithiated thiophenes 140 and 141 to dione 142. Pinacol rearrangement of the resulting diols, 143 and 144, produced ketones 145 and 146, respectively (Scheme 24a). Reduction with LiAlH<sub>4</sub>, followed by a Wagner-Meerwein-type rearrange-

**Scheme 23** (a) Synthesis of a symmetric imidazole-bridged DAE. *N*-Substitution of imidazole-bridged DAEs *via*: (b) nucleophilic substitution and (c) copper-catalyzed coupling.



**Scheme 24** (a) Synthesis of symmetric acenaphthylene-bridged DAEs. (b) Nucleophilic addition of organolithium compounds to DAEs containing acenaphthylene bridges. <sup>a</sup> BnMgBr used instead of *n*BuLi.

Scheme 25 Synthesis of DAEs possessing bicyclic bridges *via* [4 + 2] cycloaddition of a diaryl precursor with: (a) dicyanofumarate; or (b) 1-hydroxy-3-phenylthiourea in the presence of Pr<sub>4</sub>NIO<sub>4</sub>.

ment of the resulting alcohols, **147** and **148**, yielded DAEs **138** and **139**, respectively. Treating DAEs **138** or **139** with organolithium reagents and trapping with primary alkyl bromides produced photochromic DAEs **149–156** (Scheme 24b). The reactivity of DAE **138** under these conditions was unexpected, given the presence of chloro groups at the 2- and 2'-positions. The 3,4-additions to DAEs **138** and **139** proceeded with 17–58% yield, and generated the *trans* adducts, exclusively. The photochromic properties of DAE **150** were studied, and  $\phi_{\text{o-c}} = 0.49$  was measured.

The last approach we will discuss is the use of [4 + 2] cycloaddition to access non-symmetric DAEs with bicyclic bridges (Scheme 25), in which the cycloaddition products are obtained as mixtures of enantiomers. This approach has been mainly used to realize photochemical locking-unlocking of the Diels-Alder adducts. Branda and co-workers reported the synthesis of DAEs 157 and 158 via cycloaddition of DAE precursors 159 160, respectively, with diethyl dicyanofumarate (Scheme 25a). 99 Fulvenes 159 and 160 were obtained by oxidizing symmetric DAEs 161 and 162, respectively, followed by pyrrolidine-catalyzed condensation with cyclohexanone. DAEs 161 and 162 were prepared using a ring-closing strategy (see section 4.1). The closed isomers of DAEs 157 and 158 are no longer Diels-Alder adducts, and are therefore thermally stable. After photo-induced retroelectrocyclization, dienes 159 and 160 were released at room temperature. Similarly, McConville and co-workers more recently synthesized DAE 163, starting with the oxidation of symmetric DAE 164 using bromine, followed by cycloaddition of the resulting diene 165 with 1-hydroxy-3-phenylthiourea in the presence of Pr<sub>4</sub>NIO<sub>4</sub> (Scheme 25b). 100 Similar to DAEs 157 and 158, DAE 163 also exhibited photochemical locking-unlocking of the Diels-Alder adduct. The thermally released acyl nitroso dienophile may hydrolyze in the presence of water, forming nitroxyl, an active pharmacological agent. Thus, DAEs are promising scaffolds for photoswitchable drug-delivery systems. 101

#### 6. Conclusion

The unique properties of photochromic DAEs have driven the development of synthetic strategies to access DAE structures of increasing complexity. In particular, non-symmetric DAEs have gained popularity in a variety of research fields. Several strategies have been developed and adapted to access these scaffolds: coupling aryl groups to a bridge precursor, ringclosing of diaryl intermediates, and desymmetrizing a symmetric DAE or DAE precursor. While desymmetrization has enjoyed continued expansion, the development of coupling and ring-closing strategies has substantially diversified the types of non-symmetric DAEs that are accessible. The easy access to symmetric DAEs precursors has been the main advantage for desymmetrization strategies, while coupling and ring-closing strategies have mainly been used to access hybrid DAEs structures with different aryl groups, as well as unusual, functionalizible bridges. Together, these strategies have contributed to the improvement of DAE photochromic properties, and have boosted the development of photocontrolled systems.

There are several directions for continued expansion of the library of non-symmetric DAE structures and exploring their applications. So far, most non-symmetric DAE applications benefit from light-induced changes in electronic conjugation between DAE substituents, but there have been few studies that take advantage of geometric changes associated with DAE photoisomerization. Aryl group functionalization of symmetric DAEs is mostly limited to thienylic DAE substrates, but could potentially be applied to DAEs with other heteroaryl groups with similar reactivity. In addition, emerging C–H and C–F activation methods are attractive routes for DAE desymmetrization. Continued work on the structural diversification of non-symmetric DAEs using current and novel synthetic tools will help realize the full potential of DAE systems, leading to applications that will benefit from new modes of photocontrol.

### Conflicts of interest

There are no conflicts to declare.

## Acknowledgements

The authors gratefully acknowledge an NSF CAREER award (1945271) and a Turner Fellowship (Stony Brook University) to L. D. for funding.

#### Notes and references

- 1 M. Irie and M. Mohri, J. Org. Chem., 1988, 53, 803-808.
- 2 K. Zheng, S. Han, X. Zeng, Y. Wu, S. Song, H. Zhang and X. Liu, Adv. Mater., 2018, 30, 1801726.
- 3 K. Börjesson, M. Herder, L. Grubert, D. T. Duong, A. Salleo, S. Hecht, E. Orgiu and P. Samorì, J. Mater. Chem. C, 2015, 3, 4156-4161.
- 4 B. Roubinet, M. Weber, H. Shojaei, M. Bates, M. L. Bossi, V. N. Belov, M. Irie and S. W. Hell, J. Am. Chem. Soc., 2017, 139, 6611-6620.
- 5 B. M. Neilson and C. W. Bielawski, J. Am. Chem. Soc., 2012, 134, 12693-12699.
- 6 Z. Li, X. Han, H. Chen, D. Wu, F. Hu, S. H. Liu and J. Yin, Org. Biomol. Chem., 2015, 13, 7313-7322.
- 7 J. R. Nilsson, M. C. O'Sullivan, S. Li, H. L. Anderson and J. Andréasson, Chem. Commun., 2015, 51, 847-850.
- 8 D. Roke, C. Stuckhardt, W. Danowski, S. J. Wezenberg and B. L. Feringa, Angew. Chem., Int. Ed., 2018, 57, 10515-10519.
- 9 F. Eisenreich, M. Kathan, A. Dallmann, S. P. Ihrig, T. Schwaar, B. M. Schmidt and S. Hecht, Nat. Catal., 2018, 1, 516-522.
- 10 B. M. Neilson and C. W. Bielawski, Chem. Commun., 2013, 49, 5453-5455.
- 11 D. Liu, A. D. Sponza, D. Yang and M. Chiu, Angew. Chem., Int. Ed., 2019, 58, 16210-16216.
- 12 G. M. Peters and J. D. Tovar, J. Am. Chem. Soc., 2019, 141, 3146-3152.
- 13 X. Hu, M. E. McFadden, R. W. Barber and M. J. Robb, J. Am. Chem. Soc., 2018, 140, 14073-14077.
- 14 R. W. Barber, M. E. McFadden, X. Hu and M. J. Robb, Synlett, 2019, 30, 1725-1732.
- 15 M. Irie, T. Fukaminato, K. Matsuda and S. Kobatake, Chem. Rev., 2014, 114, 12174-12277.
- 16 M. Irie, Chem. Rev., 2000, 100, 1685-1716.
- 17 A. G. Lvov, Y. Yokoyama and V. Z. Shirinian, Chem. Rec., 2020, 20, 51-63.
- 18 J. Zhang and H. Tian, Adv. Opt. Mater., 2018, 6, 1701278.
- 19 S.-Z. Pu, Q. Sun, C.-B. Fan, R.-J. Wang and G. Liu, J. Mater. Chem. C, 2016, 4, 3075-3093.
- 20 A. Fihey, A. Perrier, W. R. Browne and D. Jacquemin, Chem. Soc. Rev., 2015, 44, 3719-3759.
- 21 A. Fihey and D. Jacquemin, *Chem. Sci.*, 2015, **6**, 3495–3504.
- 22 G. Szalóki and J.-L. Pozzo, Chem. Eur. J., 2013, 19, 11124-11132.

- 23 K. Uchida and M. Irie, Chem. Lett., 1995, 24, 969-970.
- 24 H. Nakashima and M. Irie, Polym. J., 1998, 30, 985-989.
- 25 H. Nakashima and M. Irie, Macromol. Chem. Phys., 1999, 200, 683-692.
- 26 S. Abe, A. Sugai, I. Yamazaki and M. Irie, Chem. Lett., 1995, 24, 69-70.
- 27 S. H. Kawai, S. L. Gilat and J.-M. Lehn, Eur. J. Org. Chem., 1999, 2359-2366,
- 28 Y. Odo, K. Matsuda and M. Irie, Chem. Eur. J., 2006, 12, 4283-4288.
- 29 H. D. Samachetty and N. R. Branda, Chem. Commun., 2005, 2840-2842.
- 30 G. Bianchini, G. Strukul, D. F. Wass and A. Scarso, RSC Adv., 2015, 5, 10795-10798.
- 31 D. Wilson and N. R. Branda, Angew. Chem., Int. Ed., 2012, **51**, 5431–5434.
- 32 S. Fredrich, A. Bonasera, V. Valderrey and S. Hecht, J. Am. Chem. Soc., 2018, 140, 6432-6440.
- 33 C. C. Warford, C.-J. Carling and N. R. Branda, Chem. Commun., 2015, 51, 7039-7042.
- 34 S. Pu, C. Zheng, Q. Sun, G. Liu and C. Fan, Chem. Commun., 2013, 49, 8036-8038.
- 35 S. Fukumoto, T. Nakashima and T. Kawai, Angew. Chem., Int. Ed., 2011, 50, 1565-1568.
- 36 S. Chen, Y. Yang, Y. Wu, H. Tian and W. Zhu, J. Mater. Chem., 2012, 22, 5486-5494.
- 37 Y. Tani, T. Ubukata, Y. Yokoyama and Y. Yokoyama, I. Org. Chem., 2007, 72, 1639-1644.
- 38 Y. Yokoyama, H. Shiraishi, Y. Tani, Y. Yokoyama and Y. Yamaguchi, J. Am. Chem. Soc., 2003, 125, 7194–7195.
- 39 M. Kose, M. Shinoura, Y. Yokoyama and Y. Yokoyama, J. Org. Chem., 2004, 69, 8403-8406.
- 40 T. Shiozawa, M. K. Hossain, T. Ubukata and Y. Yokoyama, Chem. Commun., 2010, 46, 4785-4787.
- 41 M. Hanazawa, R. Sumiya, Y. Horikawa and M. Irie, J. Chem. Soc., Chem. Commun., 1992, 206-207.
- 42 S. Cui, S. Pu and G. Liu, Spectrochim. Acta, Part A, 2014, 132, 339-344.
- 43 T. Asai, A. Takata, A. Nagaki and J.-I. Yoshida, ChemSusChem, 2012, 5, 339-350.
- 44 G. Liu, S. Pu and R. Wang, Org. Lett., 2013, 15, 980–983.
- 45 H. Nishi, T. Namari and S. Kobatake, J. Mater. Chem., 2011, 21, 17249-17258.
- 46 Y. Nakagawa, M. Morimoto, N. Yasuda, K. Hyodo, S. Yokojima, S. Nakamura and K. Uchida, Chem. - Eur. J., 2019, 25, 7874-7880.
- 47 T. Yamaguchi, M. Hosaka, T. Ozeki, M. Morimoto and M. Irie, Tetrahedron Lett., 2011, 52, 5601-5604.
- 48 C. Zheng, G. Liu and S. Pu, Tetrahedron Lett., 2013, 54, 5791-5794.
- 49 J. Liu, H. Liu and S. Pu, Tetrahedron Lett., 2015, 56, 5223-
- 50 H. Liu, S. Pu, G. Liu and B. Chen, Tetrahedron Lett., 2013, 54, 646-650.
- 51 S. M. Shrestha, H. Nagashima, Y. Yokoyama and Y. Yokoyama, Bull. Chem. Soc. Jpn., 2003, 76, 363-367.

- 52 G. Liu, M. Liu, S. Pu, C. Fan and S. Cui, *Tetrahedron*, 2012, **68**, 2267–2275.
- 53 G.-T. Xu, B. Li, J.-Y. Wang, D.-B. Zhang and Z.-N. Chen, *Chem. Eur. J.*, 2015, **21**, 3318–3326.
- 54 K. Uchida, T. Matsuoka, K. Sayo, M. Iwamoto, S. Hayashi and M. Irie, *Chem. Lett.*, 1999, 28, 835–836.
- 55 For a counterexample, see: T. Kudernac, T. Kobayashi, A. Uyama, K. Uchida, S. Nakamura and B. L. Feringa, J. Phys. Chem. A, 2013, 117, 8222–8229.
- 56 K. Uchida, T. Ishikawa, M. Takeshita and M. Irie, *Tetrahedron*, 1998, 54, 6627–6638.
- 57 S. Pu, H. Li, G. Liu and W. Liu, *Tetrahedron Lett.*, 2010, **51**, 3575–3579.
- 58 T. Nakashima, K. Atsumi, S. Kawai, T. Nakagawa, Y. Hasegawa and T. Kawai, *Eur. J. Org. Chem.*, 2007, 3212–3218.
- 59 R. Li, T. Nakashima, O. Galangau, S. Iijima, R. Kanazawa and T. Kawai, *Chem. Asian J.*, 2015, **10**, 1725–1730.
- 60 S. Fukumoto, T. Nakashima and T. Kawai, *Eur. J. Org. Chem.*, 2011, 5047–5053.
- 61 J. C.-H. Chan, W. H. Lam, H.-L. Wong, N. Zhu, W.-T. Wong and V. W.-W. Yam, J. Am. Chem. Soc., 2011, 133, 12690–12705.
- 62 J. C.-H. Chan, H.-L. Wong, W.-T. Wong and V. W.-W. Yam, *Chem. Eur. J.*, 2015, 21, 6936–6948.
- 63 M. Kose, E. Orhan, K. Suzuki, A. Tutar, C. S. Ünlü and Y. Yokoyama, *J. Photochem. Photobiol.*, *A*, 2013, 257, 50–53.
- 64 M. Singer and A. Jäschke, J. Am. Chem. Soc., 2010, 132, 8372–8377.
- 65 H. Cahová and A. Jäschke, *Angew. Chem., Int. Ed.*, 2013, 52, 3186–3190.
- 66 M. Herder, F. Eisenreich, A. Bonasera, A. Grafl, L. Grubert, M. Pätzel, J. Schwarz and S. Hecht, *Chem. – Eur. J.*, 2017, 23, 3743–3754.
- 67 C. Jurissek, F. Berger, F. Eisenreich, M. Kathan and S. Hecht, *Angew. Chem., Int. Ed.*, 2019, **58**, 1945–1949.
- 68 B. R. Beno, K.-S. Yeung, M. D. Bartberger, L. D. Pennington and N. A. Meanwell, *J. Med. Chem.*, 2015, 58, 4383–4438.
- 69 C.-T. Poon, W. H. Lam, H.-L. Wong and V. W.-W. Yam, J. Am. Chem. Soc., 2010, 132, 13992–13993.
- 70 M. H.-Y. Chan, H.-L. Wong and V. W.-W. Yam, *Inorg. Chem.*, 2016, 55, 5570–5577.
- 71 L. N. Lucas, J. van Esch, R. M. Kellogg and B. L. Feringa, Tetrahedron Lett., 1999, 40, 1775–1778.
- 72 V. A. Migulin, M. M. Krayushkin, V. A. Barachevsky, O. I. Kobeleva, T. M. Valova and K. A. Lyssenko, *J. Org. Chem.*, 2012, 77, 332–340.
- 73 N. B. Zuckerman, X. Kang, S. Chen and J. P. Konopelski, *Tetrahedron Lett.*, 2013, 54, 1482–1485.
- 74 V. Z. Shirinian, A. A. Shimkin, D. V. Lonshakov, A. G. Lvov and M. M. Krayushkin, *J. Photochem. Photobiol.*, A, 2012, 233, 1–14.
- 75 V. Z. Shirinian, A. G. Lvov, M. M. Krayushkin, E. D. Lubuzh and B. V. Nabatov, *J. Org. Chem.*, 2014, 79, 3440–3451.
- 76 A. G. Lvov, E. Y. Bulich, A. V. Metelitsa and V. Z. Shirinian, RSC Adv., 2016, 6, 59016–59020.

- 77 A. G. Lvov, A. M. Kavun, V. V. Kachala, Y. V. Nelyubina, A. V. Metelitsa and V. Z. Shirinian, *J. Org. Chem.*, 2017, 82, 1477–1486.
- 78 J. C.-H. Chan, W. H. Lam and V. W.-W. Yam, *J. Am. Chem. Soc.*, 2014, **136**, 16994–16997.
- 79 N. M.-W. Wu, H.-L. Wong and V. W.-W. Yam, *Chem. Sci.*, 2017, 8, 1309–1315.
- 80 B. Wu, M. Santra and N. Yoshikai, *Angew. Chem., Int. Ed.*, 2014, 53, 7543–7546.
- 81 N. M.-W. Wu, M. Ng, W. H. Lam, H.-L. Wong and V. W.-W. Yam, *J. Am. Chem. Soc.*, 2017, **139**, 15142–15150.
- 82 S. Iijima, T. Nakashima and T. Kawai, New J. Chem., 2016, 40, 10048–10055.
- 83 K. Morinaka, T. Ubukata and Y. Yokoyama, *Org. Lett.*, 2009, **11**, 3890–3893.
- 84 Z. Xu, Y. Cao, B. O. Patrick and M. O. Wolf, *Chem. Eur. J.*, 2018, 24, 10315–10319.
- 85 T. Nakagawa, Y. Miyasaka and Y. Yokoyama, *Chem. Commun.*, 2018, **54**, 3207–3210.
- 86 R. Göstl, B. Kobin, L. Grubert, M. Pätzel and S. Hecht, *Chem. Eur. J.*, 2012, **18**, 14282–14285.
- 87 Y. Liang, W. Geng, J. Wei and Z. Xi, *Angew. Chem., Int. Ed.*, 2012, **51**, 1934–1937.
- 88 Y.-R. Chen and W.-L. Duan, J. Am. Chem. Soc., 2013, 135, 16754–16757.
- 89 L. N. Lucas, J. J. D. de Jong, J. H. V. Esch, R. M. Kellogg and B. L. Feringa, *Eur. J. Org. Chem.*, 2003, 155–166.
- 90 K. Higashiguchi, G. Taira, J.-I. Kitai, T. Hirose and K. Matsuda, J. Am. Chem. Soc., 2015, 137, 2722–2729.
- 91 H. Kamiya, S. Yanagisawa, S. Hiroto, K. Itami and H. Shinokubo, *Org. Lett.*, 2011, **13**, 6394–6397.
- 92 Y.-C. Jeong, D. G. Park, E. Kim, K.-H. Ahn and S. I. Yang, Chem. Commun., 2006, 1881–1883.
- 93 R. Kodama, K. Sumaru, K. Morishita, T. Kanamori, K. Hyodo, T. Kamitanaka, M. Morimoto, S. Yokojima, S. Nakamura and K. Uchida, *Chem. Commun.*, 2015, 51, 1736–1738.
- 94 S. Li, R. Liu, X. Jiang, Y. Qiu, X. Song, G. Huang, N. Fu, L. Lin, J. Song, X. Chen and H. Yang, ACS Nano, 2019, 13, 2103–2113.
- 95 B. Verbelen, E. Siemes, A. Ehnbom, C. Rauber, K. Rissanen, D. Woll and C. Bolm, *Org. Lett.*, 2019, 21, 4293–4297.
- 96 G. Duan and V. W.-W. Yam, *Chem. Eur. J.*, 2010, **16**, 12642–12649.
- 97 G. Duan, W.-T. Wong and V. W.-W. Yam, *New J. Chem.*, 2011, 35, 2267–2278.
- 98 C. Lambruschini, L. Banfi and G. Guanti, *Chem. Eur. J.*, 2016, 22, 13831–13834.
- 99 V. Lemieux, S. Gauthier and N. R. Branda, *Angew. Chem., Int. Ed.*, 2006, **45**, 6820–6824.
- 100 K. P. Schultz, D. W. Spivey, E. K. Loya, J. E. Kellon, L. M. Taylor and M. R. McConville, *Tetrahedron Lett.*, 2016, 57, 1296–1299.
- 101 A. M. Asadirad and N. R. Branda, *J. Am. Chem. Soc.*, 2015, 137, 2824–2827.